N94-35295

INTERNATIONAL SPACE STATION ALPHA'S BEARING, MOTOR, AND ROLL RING MODULE DEVELOPMENTAL TESTING AND RESULTS

David L. O'Brien
Rocketdyne Division
Rockwell International
Canoga Park, California

ABSTRACT

This paper presents the design and developmental testing associated with the bearing, motor, and roll ring module (BMRRM) used for the beta rotation axis on International Space Station Alpha (ISSA). The BMRRM with its controllers located in the electronic control unit (ECU), provides for the solar array pointing and tracking functions as well as power and signal transfer across a rotating interface.

INTRODUCTION

The BMRRM is part of the beta gimbal assembly (BGA), as shown in Figure 1. The BMRRM is located between the beta gimbal transition structure (which deploys the BGA and solar array away from the station) and the BGA platform. The sequential shunt unit, ECU and solar array are all attached to the BGA platform.

The beta rotation axis is the second of two axes required to allow maximum use of solar power for the electrical systems aboard the space station. The beta axis servocontrol compensates for both the seasonal and orbital changes in the station's orientation to the solar vector (line-of-sight). Under the ISSA program, nominal beta axis rotational rates vary from zero to 0.096 rad/d (five degrees per day). Shuttle docking (plume loads) and extravehicular / intravehicluar operations also define expected beta axis motions. The maximum allowable velocity is 0.076 rad/s (240 degrees per minute), although the default control parameters limit velocity to 0.025 rad/s. The beta gimbal was designed under the Space Station Freedom requirements, which had an additional requirement of alpha axis rotation in early flights, which is around 0.078 rad/min, (four degrees per minute). The leading design drivers of the BMRRM are the beta axis servocontrol, power and signal transfer through a rotating joint, and structural loading requirements. Small angle oscillations are also expected due to vibrational modes of the station.

BMRRM DESIGN

The BMRRM consists of two sets of angular contact bearings, a brushless dc torque motor, resolver, roll ring subassembly, antirotation latches, and a housing to hold the components together. The electronics to operate the motor, latches, and resolver are located in the ECU. A cross-sectional view of the BMRRM is shown in Figure 2. The bearings, motor, and roll ring are all concentric to each other. The

BMRRM's total mass is 63.5 kg, of which the roll ring is 27.2 kg, the motor 8.2 kg, and the bearings 5.4 kg.

The angular contact bearings provide structural stiffness about five axes. The bearing sets are separated by 0.5 m (20 inches), which accommodates bending loads. The outboard bearing set (toward the solar array) supports axial loading. The inboard set is free to move axially to accommodate thermal expansion and tolerance stacking. Each bearing set was consists of two 0.45 m diameter angular contact bearings mounted face-to-face and preloaded to 0.34 rad (18 degrees) contact angle.

A brushless dc motor provides the torque about the beta axis. Due to the low required torque of 1.4 N-m (12 in-lb) plus friction losses (less than 2 N-m), a direct drive motor was used. Eliminating a geared system helped pointing accuracy by reducing frictions losses, thus reducing station vibration disturbances on the inertially stable array. Eliminating the geared system also helped control stability by abolishing backlash, reduced power consumption due to lower frictions losses, reduced mass, and increased life (no gear wear). The motor is capable of providing 45 N-m torque (stall), resulting in about 8 to 1 torque margin. The motor is a 3-phase, Y-wound, 64-pole device about 0.4 m in diameter. Figure 3 shows an outboard view of the BMRRM with the motor and roll ring connector.

The resolver, which is located within the roll ring subassembly, provides arc-minute pointing accuracy knowledge for the proportional-integral-derivative (PID) closed servoloop. The PID servoloop is a digital controller located in the ECU. The BGA/BMRRM does not use inertia or solar sensing instruments. The pointing control comes from the station's guidance, navigation, and control system or the ground, via the photovoltaic controller unit. As a backup, the motor and controller are designed to allow open-loop stepping. The resolver pointing knowledge is also used for commutating the motor.

The roll ring subassembly provides bidirectional transfer of source power (212 A), secondary and dc control power (less than 8 A) and MIL-STD-1553B data signals. The roll ring, as being installed into the BMRRM, is shown on Figure 4. The transfer is across a rotating joint through slightly compressed multiple rotating flexures connecting the inner and outer conducting rings. The rotating flexures greatly reduce the sliding friction, allowing the BMRRM to be rotated with very low torques. Most of the BMRRM's torsional friction comes from the angular contact bearings.

There are two antirotation latches in the BMRRM each 1.77 rad (92.8125 degrees) apart. There are 64 holes in the BMRRM housing flange; therefore, by oscillating between the latches, 128 latching positions are available (every 0.05 rad or 2.8125 degrees). An antirotation latch is a paraffin actuated pull-pin device. When 15 Vdc power is applied by the ECU the paraffin solid-to-liquid phase change results in pulling the pin out of the latch hole and resets a toggle mechanism. The next time power is applied the paraffin actuator toggles the mechanism and allows the spring loaded pin to be pushed back into the latching hole.

The BMRRM can be replaced on-orbit. To facilitate this the roll ring contains a single input mating connector as shown in Figure 3. This connector includes all power, motor, latch, and resolver lines.

BMRRM TESTS AND RESULTS

Four series of tests were performed: component functional, system functional, thermal vacuum, and static structural. Both functional tests were performed in a clean room environment at Rocketydne, Rockwell International, Chatsworth facility. The thermal vacuum test was performed at Martin Marietta Aerospace, Denver. The static structural test was performed at Rocketydne, Rockwell International, Canoga facility. At the time of writing, 60 percent of the component and system functional tests were completed. The static structural test was fully completed. Results of the thermal vacuum and remaining functional tests will be presented at the conference.

Component Functional

The purpose of component functional testing was to verify the BMRRM design, ensure BMRRM assembly workmanship, verify the control model's component subroutines, and verify some component performance requirements. Component functional testing included friction, open-loop servo and position knowledge accuracy. The BMRRM was installed onto an electrical test set, as shown in Figure 5. The test set contained a torque cell, an external motor to rotate the BMRRM, motor voltage sensors, motor current sensors, and a motor controller (which simulates the ECU). The buildup and test sequence of the BMRRM is shown on Figure 6.

The friction tests measured the resulting torque of the main bearings, roll ring bearings, and motor clogging under several conditions. Conditions included constant velocity tests, initial torque tests, small angle dither tests, and open-loop sine wave voltage inputs. Due to the low rotational rates the BMRRM exhibited little viscous friction characteristics. Three rates were tested over a complete revolution: 0.076, 0.57, and 6.9 rad/min (4, 30, and 360 degrees per minute). The average steady-state friction torque for the three rates were 1.2, 1.3, and 1.9 N-m, respectively. However, over an operating range of zero to 0.078 rad/min the steady-state friction changes less then 1 percent. The small angle and initial torque tests show that there was no static friction involved. The friction closely resembles the Dahl model with a Dahl slope of 565 N-m/radian and a steady state torque between 1.1 and 1.8 N-m. Figure 7 compares the Dahl model and the friction test data for a 6.9 rad/min case. The friction "overshoot" shown was probably caused by motor static torque, which includes cogging as well as hysteresis effects. When the motor was tested independently a 1 N-m static friction was measured. Test set dynamics may also play a part in this overshoot, details of which will be presented at the conference.

Open-loop servo tests included back electromotive force (BEMF) and torque motor constant. The BEMF test measured the voltage outputs of each phase while the BMRRM was rotated at a constant 5.74 rad/m rate. The BEMF curves analysis will be presented at the conference. The data will state the amount of torque ripple caused by the motor. The torque motor constant test verifies controller motor power train, that is (1) motor torque, (2) motor to controller alignment, and (3) the controller current regulator. Prior to performing the torque motor constant test, the motor was aligned to the resolver by applying current through the +C -B phases. The windings were then rotated such that torque went to its stable zero (with constant current through the given phases, the windings have a sinusoidal torque curve with two zero torques, one stable and one unstable). As shown in Figure 8, the torque constant test was within 2 percent of the theoretical maximum value.

Position pointing accuracy and related alignment tests verified the pointing knowledge requirements and provided the needed accuracy for commutating the brushless motor. Position accuracy tests to measure resolver accuracy over a revolution range in both rotating directions were performed. Figure 9 shows a typical resolver error plot. The resolver "zero" is adjusted mechanically to the alignment support equipment zero. The sinusoidal error is typical for resolvers and since the error is repeatable it can be biased within the controller software.

System Functional

System functional testing included proportional hold, step inputs, rate inputs, and latching. The latter three required the use of an inertia simulator. This support equipment simulates the large inertia (8200 kg m^2) and dynamic modes of the solar array, via electrical-mechanical means. At the time of writing the inertia simulator was not complete, thus no rate or latching tests and only limited step tests were performed. These tests will be completed prior to the conference and presented thereupon.

For the proportional hold test the BMRRM was locked down at a specific position and then commanded to move to various positions. Since only the proportional constant is used, the torque produced was proportional to the constant and the error angle: $T = K_t P (\Phi_{cmd} - \Phi_{actual})$. Figure 10 shows results for several command angles and two proportional constants. As shown the system is very linear, within 2 percent.

The step tests varied from 0.0025 degrees (typical for beta rotation) to as large as 180 degrees (faulted conditions), although 5 degrees and 30 degrees steps were the baseline testing conditions. These step tests only used the hardware itself as an inertia (less than 1/3000 th of the solar array inertia), thus the system reacted abruptly to the step inputs, often exceeding velocities expected on-orbit (peaked at 1000 degrees per minute). Three control algorithms were tested: proportional (P), proportional-derivative (PD), and proportional-integral-derivative (PID). A firmware error was discovered in the integral subroutine, thus the PID reacted similar to a PD controller. The P controller test data is compared to the simulation model in Figure 11. Generally the simulation models correlate to the test data within 50 percent. It is uncertain why the model deviates from the test data points, although two reasons have been proposed: (1) the friction model is invalid at the higher speeds and (2) the modeled hardware inertia was an assumption. The PD controller test data is compared to the simulation model in Figure 12. In the PD controller case, the simulation model correlated to the test data within 30 percent. The maximum velocity for the PD controller was below the terminal velocity (which is 1.5 A divided by the derivative coefficient for a frictionless system), which validated the speed control capabilities of this positional controller.

Environmental Testing

Static structural testing was performed to verify the stress and load-deflection models. The tests represented about 75 percent of the on-orbit bending loads and 400 percent of the on-orbit torsional and shear loads. The bending loads are the main structural design driver. The BMRRM has very large torsional and shear safety factors, thus the 400 percent loading was required to amplify the deflection. Within the BMRRM the deflections generated were within 20 percent of expected values. No structural failures occurred.

Thermal vacuum/thermal balance (TVTB) testing was used primarily to verify the thermal math models. A hot and cold soak as well as transient test (emulating the 60 minute solar, 30 minute eclipse cycle) was performed. Two infrared heat lamp cages were utilized; one representing the solar flux, and the other, on the anti-solar side, representing an averaged albedo and earth IR flux. The TVTB testing showed warm BMRRM internal temperatures during the cold condition, around 5 to -13 C. Internal BMRRM hardware temperatures are limited to about -65 C. The initial design concern was that the internal temperatures may become too cold, thus a high absorptivity black painted surface was chosen. However, this 50 C margin will allow the design team to proceed with a less costly and more durable clear anodizing surface, rather than the baseline black painted surface. A 30 degree step test was planned for the ambient-ambient pressure, ambient-vacuum, cold-vacuum, and hot-vacuum conditions to measure thermally and vacuum caused differences in the servoloop. The ambient-vacuum test was successful, showing little difference between it and the ambient pressure test. However, an open developed in the B motor phase during the cold-vacuum case, which never closed even after the hardware was brought back to ambient temperature and pressure conditions. At the time of writing, the BMRRM has not been disassembled to determine where the open occurred. A step test using an external power supply and two of the three motor phases was performed during the cold-vacuum condition, although analysis is not yet complete.

CONCLUSIONS

All development testing program goals were accomplished, including:

1. The assembly and test sequence of Figure 6 was shown to be an acceptable hardware flow.
2. All component-level performance requirements were met, with the exception of the motor line open during cold thermal-vacuum testing. Once the root cause of the open is found a small design modification may be needed.
3. The system-level performance test results were within the tolerances expected, however additional testing with an inertia simulator is needed.
4. Data from the tests largely verify the control model's component friction, motor, and controller subroutines. Some additional minor friction testing is desirable to determine the cause of and model for small angle movements.
5. Data from both the static structural and thermal testing is approximate to what was expected.

Overall the BMRRM has proven to be a very tolerant, lightweight, high-accuracy rotating gimbal with minimal friction torque, and thus high rotating efficiency.

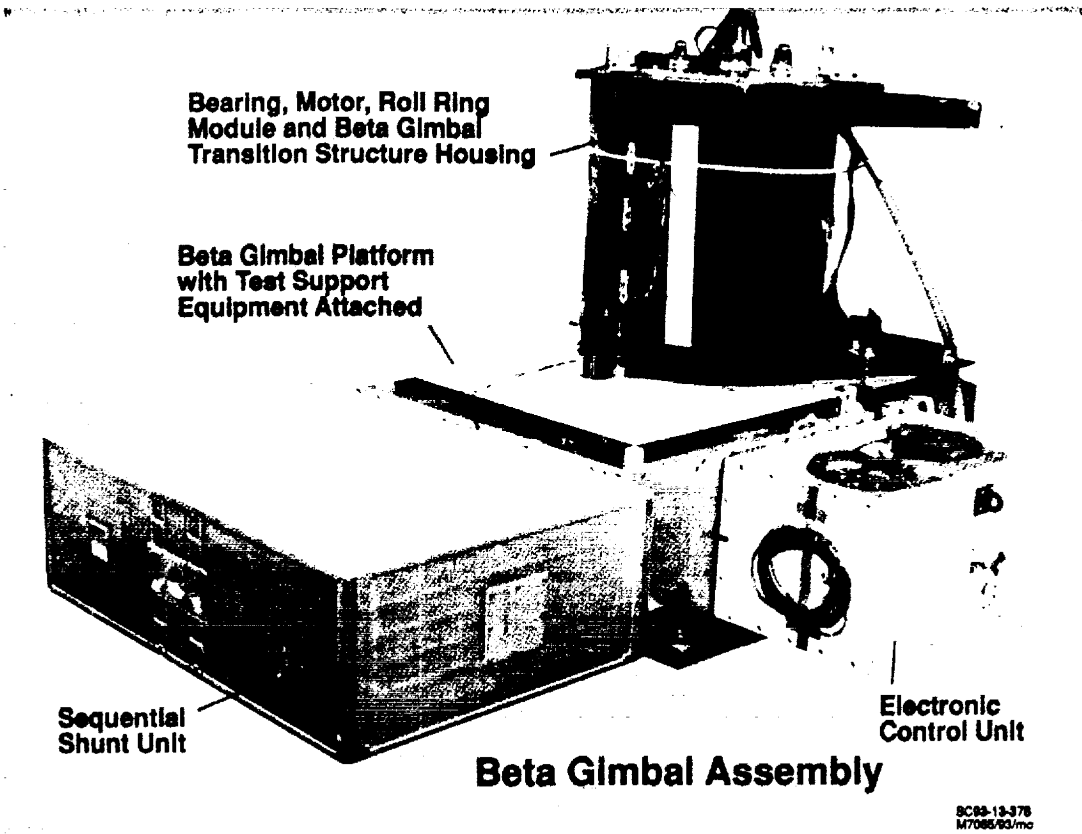

Figure 1. Beta Gimabal Assembly

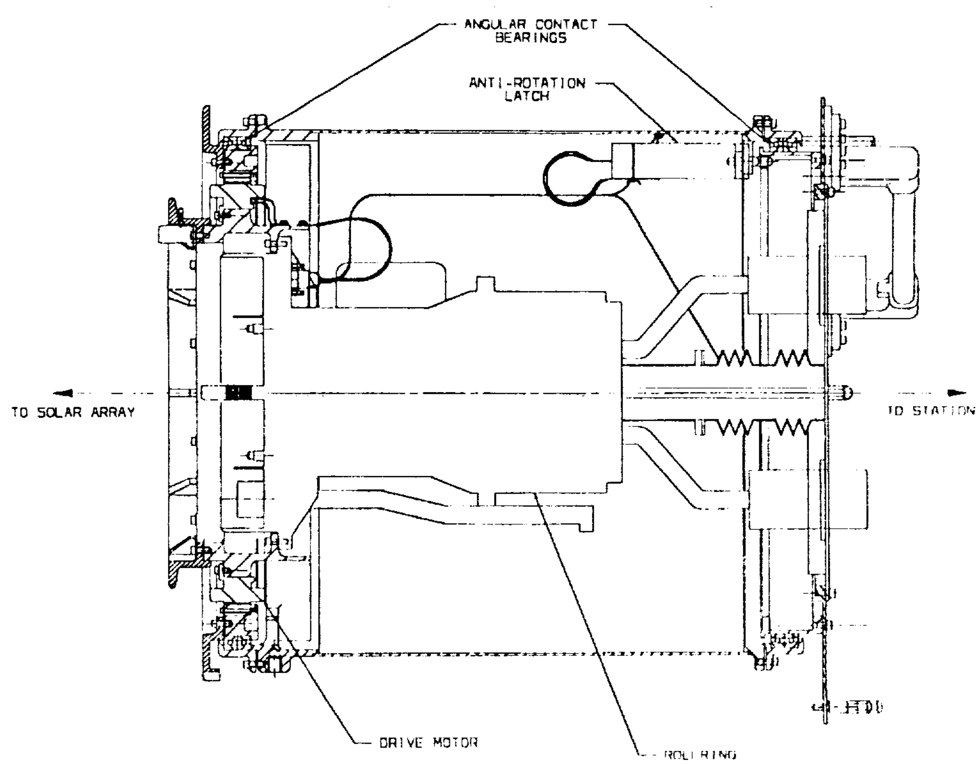

Figure 2. BMRRM Cross-sectional View

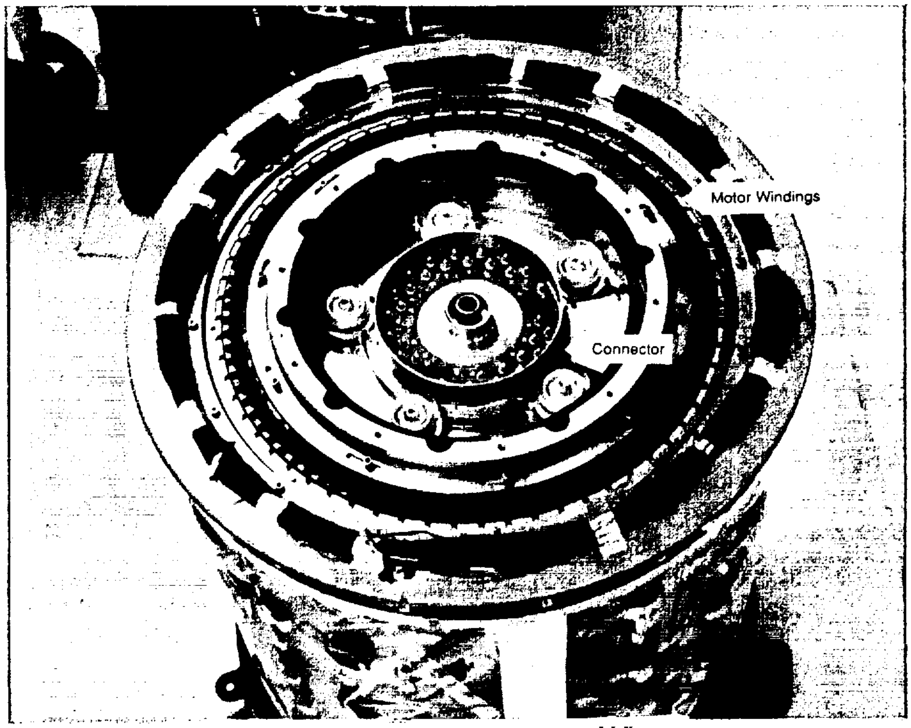

Figure 3. BMRRM Outboard View

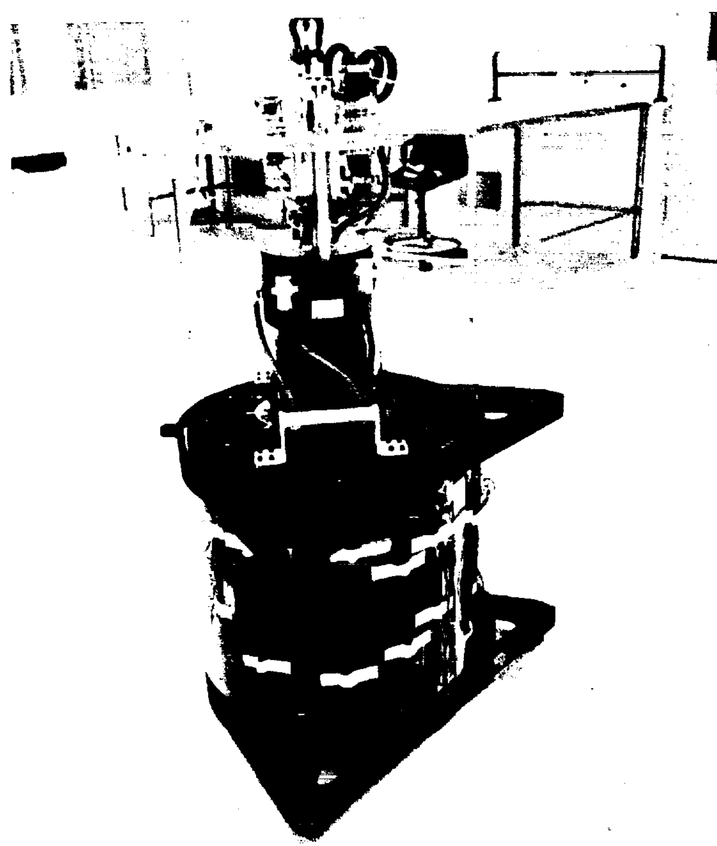
Figure 4. Roll Ring Installation into BMRRM

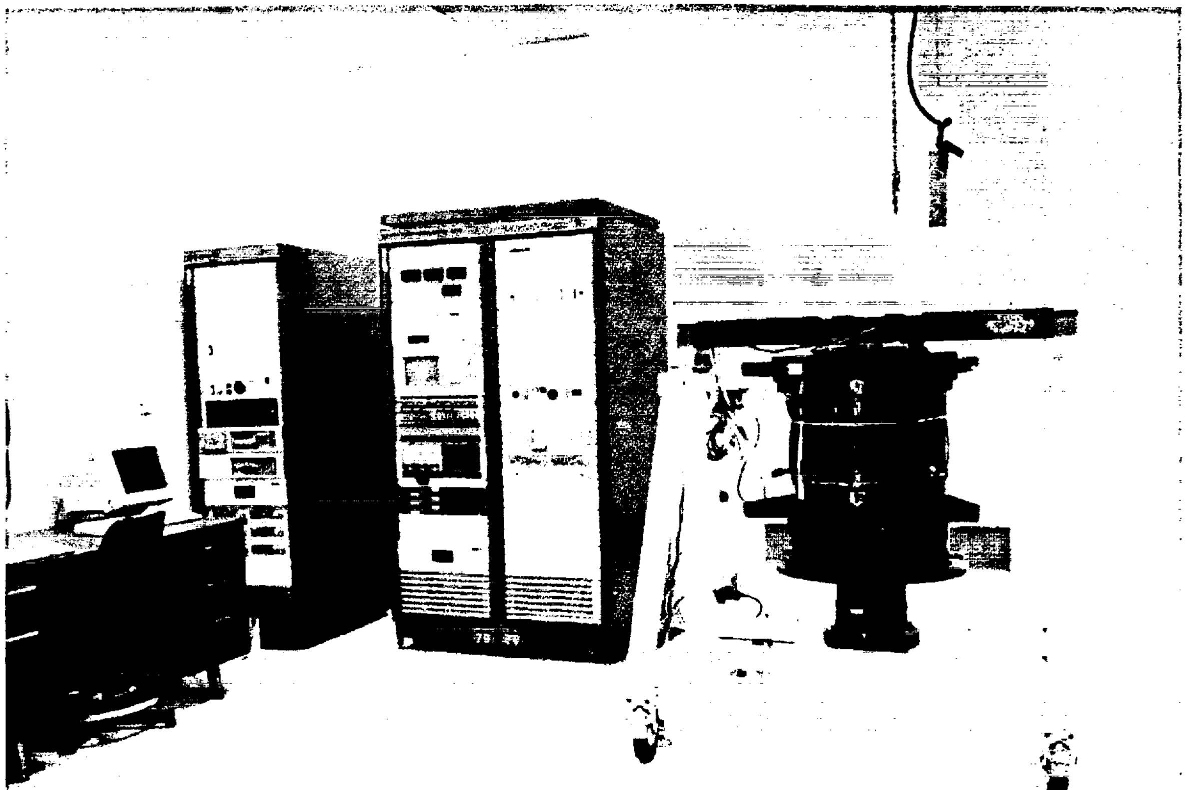

Figure 5. Electrical Functional Test Set

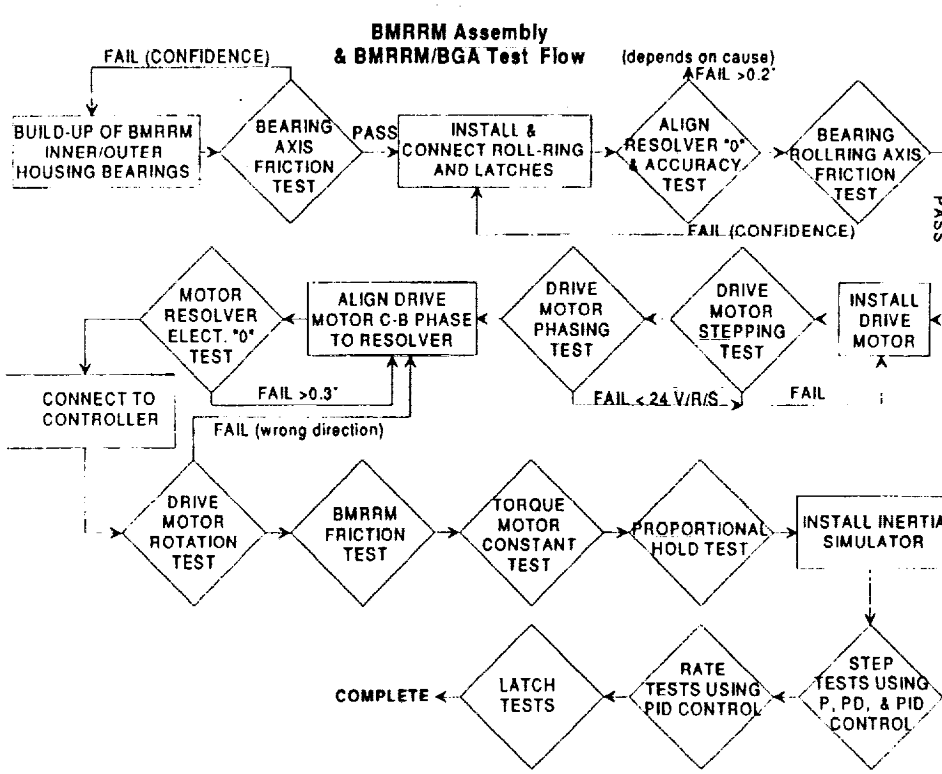

Figure 6. BMRRM Build-up and Test Sequence

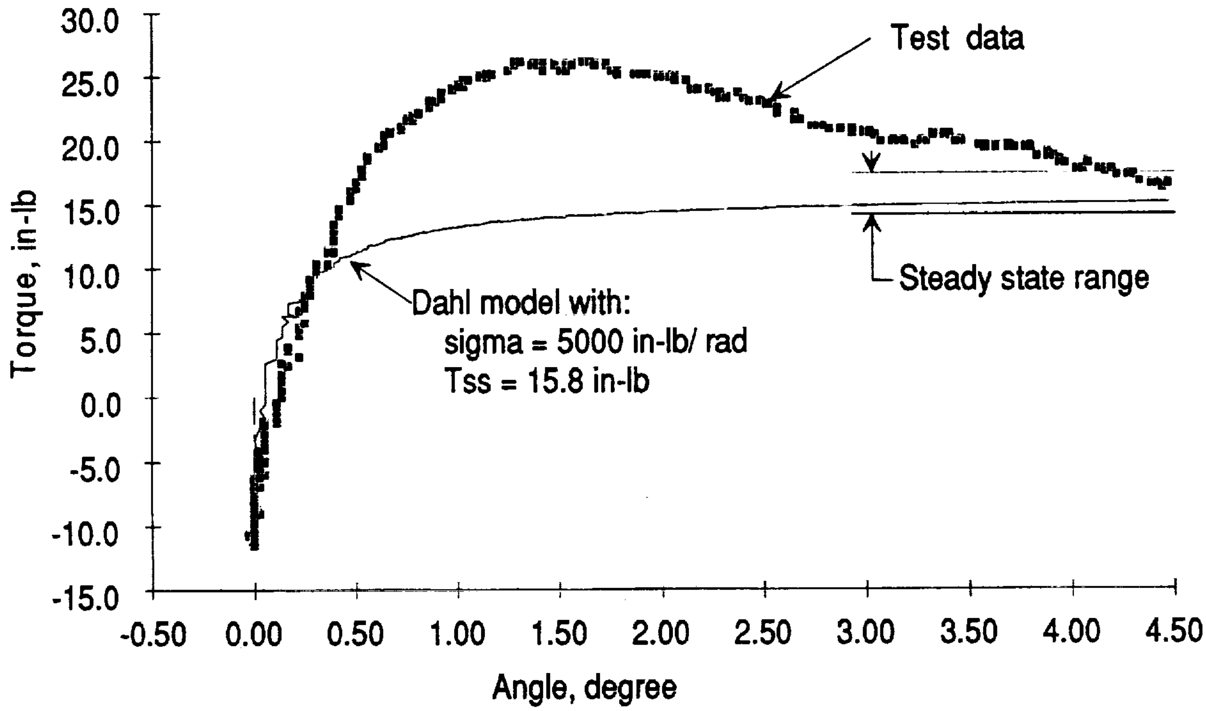

Figure 7. Typical Small Angle Friction Curve. Plot for a 360 degree per minute test.

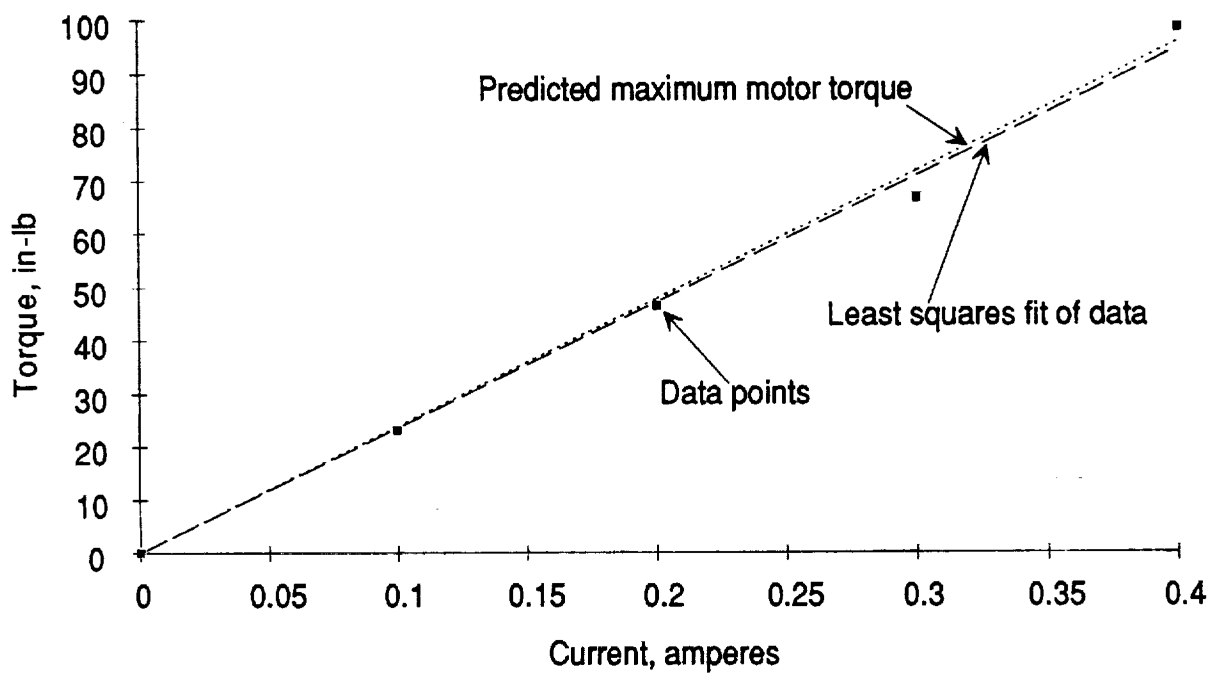

Figure 8. Torque Motor Constant Test

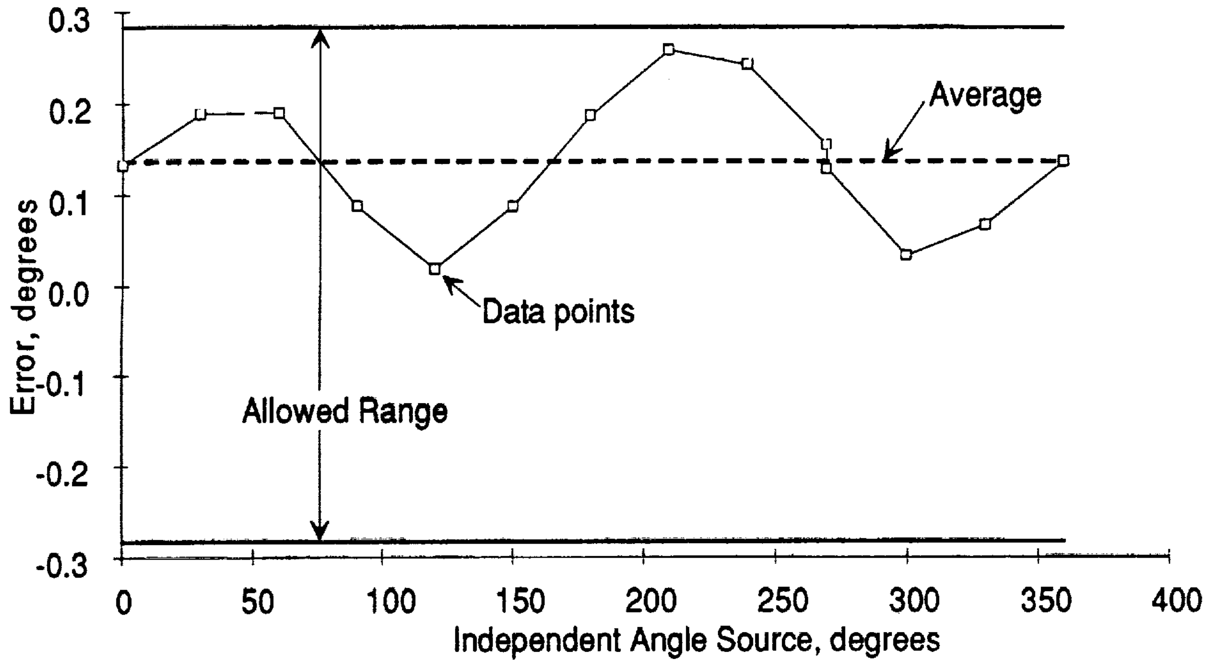

Figure 9. Resolver Accuracy Test

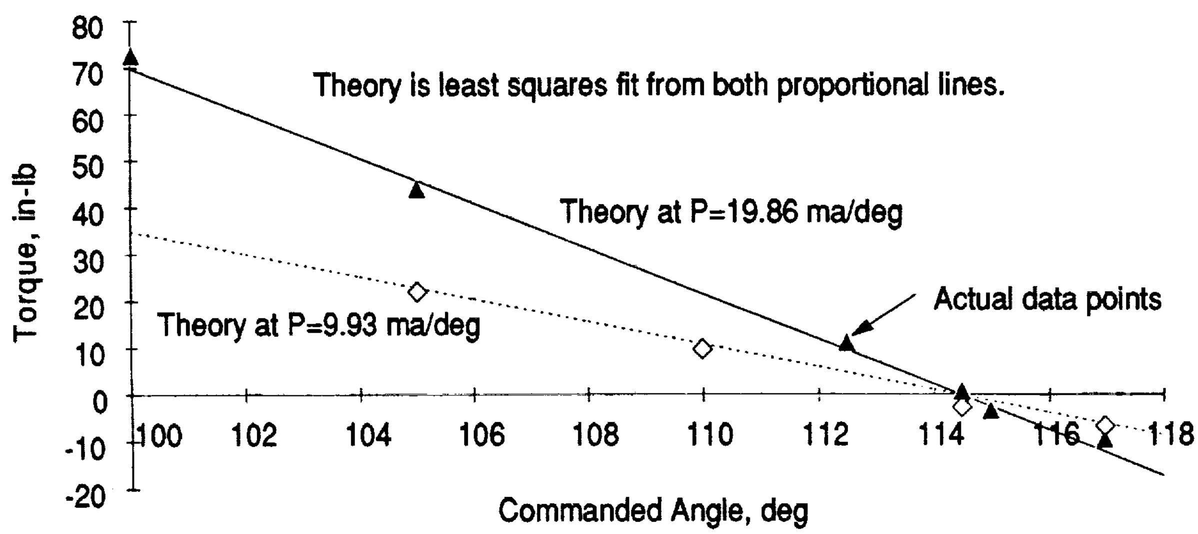

Figure 10. Proportional Hold Test

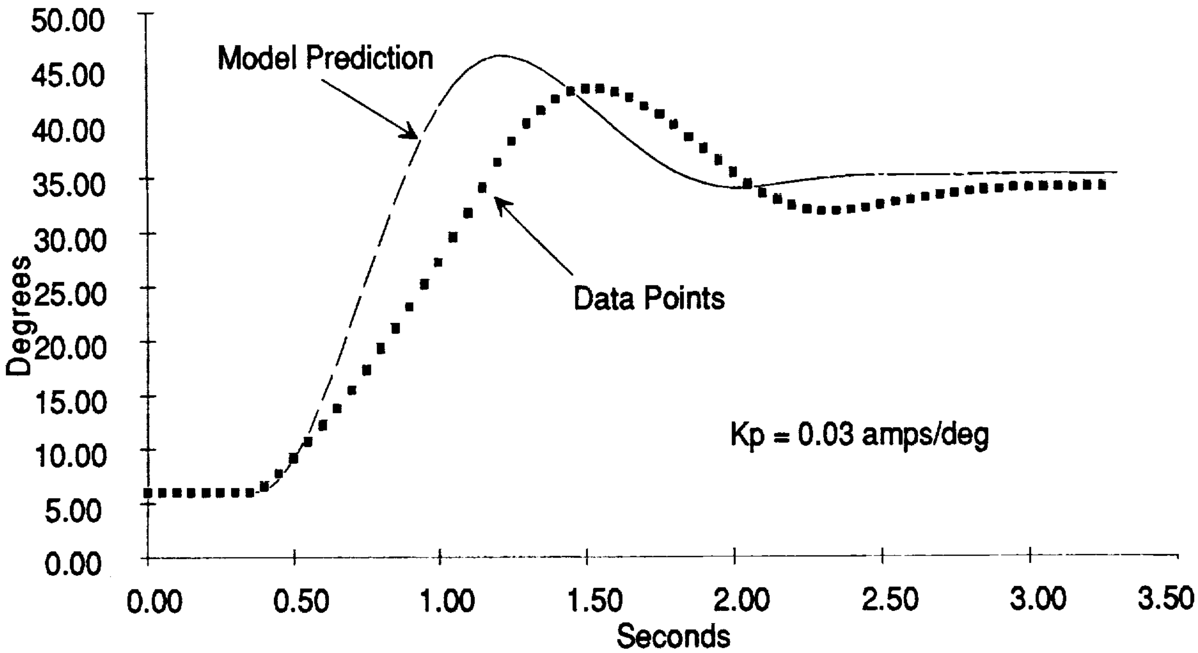

Figure 11. 30 Degree Step Input with Proportional Only Controller

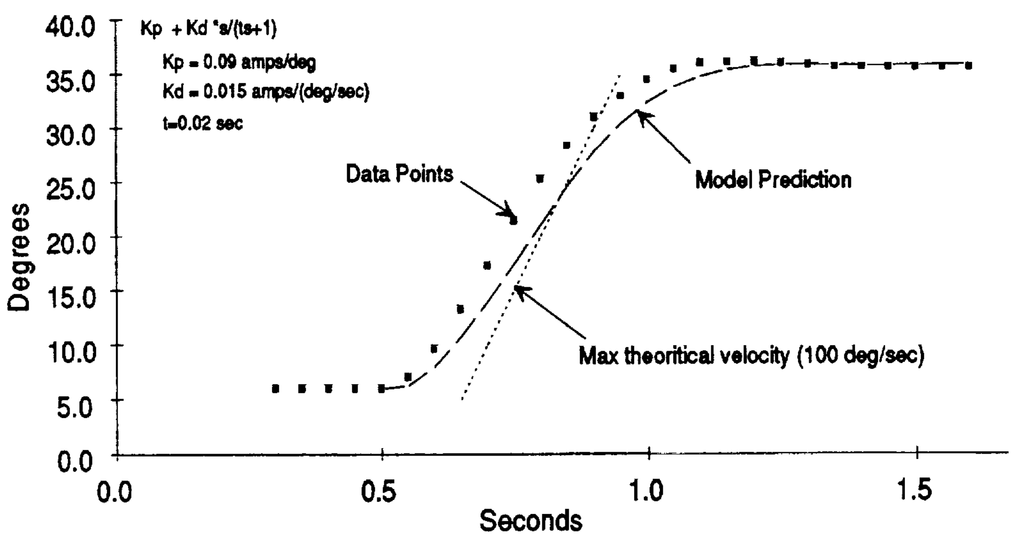

Figure 12. 30 Degree Step Input with Proportional-Derivative Controller